An Economical Procedure for Cartesian Interpolation and Display of Reflectivity Factor Data in Three-Dimensional Space[1]

C. G. MOHR AND R. L. VAUGHAN

National Center for Atmospheric Research,[2] Boulder, CO 80307

(Manuscript received 25 September 1978, in final form 31 January 1979)

ABSTRACT

A fast and efficient procedure has been developed which allows the systematic interpolation of digital reflectivity data from radar space into Cartesian space. The algorithm is designed so that only one ordered pass through the original PPI scan data is necessary to complete the interpolation process. As a result, 100 cross sections may be interpolated and displayed for approximately five times the cost of producing PPI plots for the same volume. Computer-generated displays produced by the system include contoured and gray-scale plots of orthogonal sections and perspective images of two- and three-dimensional reflectivity surfaces.

1. Introduction

The need for economical and accurate presentations of equivalent radar reflectivity (Z_e) data in an orthogonal coordinate system has existed for some time. Early attempts to simplify the display and interpretation of radar data collected in PPI scan mode include the production of constant altitude PPI's (CAPPI's) as developed by Marshall (1957) and Kessler and Russo (1963). Recent technological developments in data acquisition and computer hardware have enabled researchers to design numerous schemes for three-dimensional interpolation of data collected in spherical polar coordinate systems. Some techniques depend on collecting the data in a specialized fashion (Boardman and Smith, 1974). Others require the capability for elaborate filtering and data handling such as those schemes developed for the processing of multiple-Doppler data (Miller and Strauch, 1974; Heymsfield, 1976; Lhermitte and Gilet, 1976; Kohn *et al.*, 1978; Ray *et al.*, 1978). Despite these advances, the need for efficient techniques to reduce and display large amounts of digitized reflectivity factor data still persists. In response to this need, a simple and economical scheme has been developed for the systematic conversion of digitized Z_e estimates, which have been collected in PPI mode, to a three-dimensional Cartesian grid system. This paper describes the design and performance of a software package which has been implemented on the NCAR Control Data Corporation (CDC)/7600 for this purpose.

2. Description of the data

The data used in this procedure consist of S-band radar reflectivity factors collected in PPI scan mode by the CP-2 radar located near Grover, Colorado. The CP-2 weather radar was used in the National Hail Research Experiment (NHRE) for both operational and research applications in the study of severe convective storms. Details regarding the hardware and acquisition systems have been summarized by Eccles (1975).

The magnetic tapes containing the data are produced at the Grover site using a NOVA minicomputer. Reflectivities are available for 200 range gates spaced 0.6 km along each beam, with variable azimuth and elevation spacing, usually about 1°. Occasionally, when a storm is close to the radar, angular spacing is increased to ensure complete scanning in a reasonable period of time. In general, 2 min are required to scan the volume of a storm, with an average of 8 to 15 sector scans collected during that period.

3. Design of the software system

a. Basic requirements

The following four criteria have been stressed during the development of the system. All are interrelated and considered equally important:

1) The program package must be able to process

[1] An earlier version of this paper appeared in the *Preprints of the 18th Radar Meteorology Conference*, Atlanta, March 1978, sponsored by the American Meteorological Society.

[2] This research was performed as part of the National Hail Research Experiment managed by the National Center for Atmospheric Research and sponsored by the Weather Modification Program, Research Applications Directorate, National Science Foundation.

0021-8952/79/050661-10$06.50

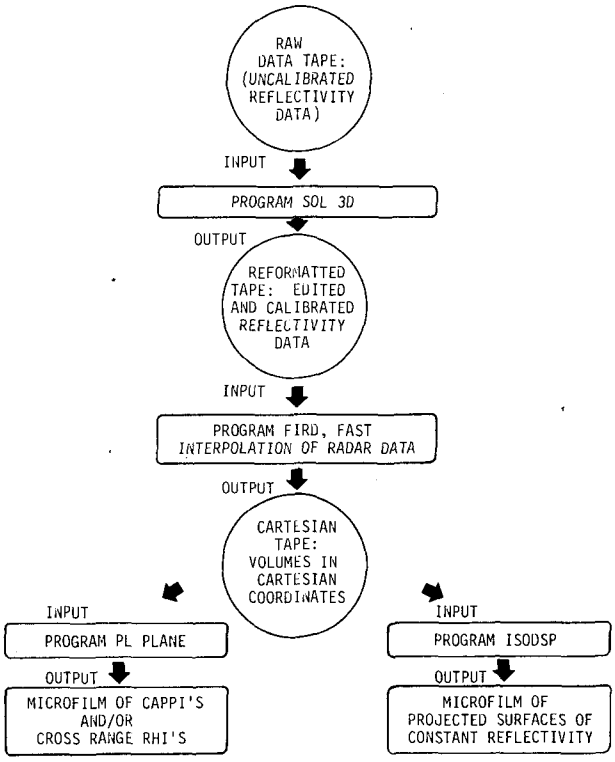

FIG. 1. Flow chart of the Cartesian interpolation and display software system.

large amounts of reflectivity data collected in PPI scan mode.

2) Computational methods must be efficient with regard to the allocation of storage and expenditure of computer time.

3) The spatial features of the original data must be preserved in Cartesian space with a minimum of smoothing.

4) The software package should be easy to use. Anyone equipped with the supporting documentation should be able to master the processing procedures with a minimum of effort.

b. Structure

Fig. 1 illustrates the structure and components of the system developed to satisfy the above requirements. Tapes containing raw data are processed by the program SOL 3D. Its function is to create a magnetic tape containing edited data in a compacted format consisting of calibrated reflectivity factors from a designated region of interest. SOL 3D also tabulates housekeeping information required by the interpolation program and places this information on the output tape ahead of the data from each storm volume scanned. Tapes produced by SOL 3D are used as input to the interpolation program (FIRD) which in turn generates tapes containing interpolated reflectivity values (dBZ) ordered along the orthogonal planes (constant z, constant y and constant x) of a specified Cartesian grid. These final tapes are then used by the display software.

Various features within the above structure can be identified as contributing to the efficiency and flexibility of the system. By saving the edited and calibrated values of Z_e it is possible to reinterpolate scanned volumes at various densities and locations within an area of interest without having to repeat initial reduction procedures using the raw data tapes. Additionally, the elimination of superfluous data and the use of a compressed format minimize the number of tapes needed to save the data required for interpolation. Similarly, the storage on magnetic tape of interpolated values permits the independent development and production of displays without unnecessary reinterpolation and data manipulation.

4. Cartesian interpolation

The most time-consuming aspect of radar data interpolation techniques tends to be the effort required to retrieve the original data needed for interpolation at a given location. This expenditure has been minimized by the implementation of a three-step procedure which enables calculation of interpolated values at all Cartesian grid-point locations while having to search through the reflectivity data, as it was originally collected, only once.

a. Outline of the interpolation procedure

The following is a general outline of the interpolation procedure.

STEP 1

The desired Cartesian coordinate system is defined and all (x,y,z) grid locations are converted to R (slant range), θ (azimuth) and ϕ (elevation) space according to the relations

$$R=(x^2+y^2+z^2)^{\frac{1}{2}}, \tag{1}$$

$$\theta=\tan^{-1}\left(\frac{x}{y}\right), \tag{2}$$

where the radar is at the origin.

Standard adjustments are made in the computation of the elevation angle ϕ to account for earth's curvature and beam refraction. The height of a given point (x,y,z) above the perceived horizon (z_h) of the radar is computed from

$$z_h=z-\frac{x^2-y^2}{iD}, \tag{3}$$

where i is the standard compensating factor (4/3) for beam refraction in the troposphere, taken from Battan (1973), and D is the diameter of the earth at the radar

site (12 810 km). ϕ is then computed as

$$\phi = \sin^{-1}\frac{z_h}{R}. \quad (4)$$

As described earlier, housekeeping information is stored on the magnetic tapes prior to the reflectivity data from each storm volume scanned. Included in this information are the elevation angles for each sector scan. Knowledge of these angles permits the calculation of an additional quantity for each Cartesian grid point called the "level number."

The volume in space bounded by two consecutive elevation scans is defined as an "interpolation level" and all Cartesian grid points contained within this volume are assigned a unique level number. Those points bounded by the first and second elevation scans are assigned a level number equal to 1. Points between the second and third scans are assigned a level number equal to 2, and so on. Cartesian grid points not contained within the total volume scanned by the radar are given a special value which later allows those points to be excluded from the interpolation process. A 60-bit computer word is then constructed with the following parameters (packed in decreasing order of significance): 1) level-number; 2) azimuth (ϕ); 3) range (R); 4) elevation (ϕ); and 5) original indices of the grid-point location in Cartesian space.

Finally, after all Cartesian grid points have been processed, the array containing the above words is sorted in ascending order.

This packing and sorting procedure reorganizes all Cartesian grid-point locations according to their interpolation level. Furthermore, it should be observed that within each interpolation level these grid-point locations will be ordered along azimuth. Having restructured the Cartesian grid system in this manner, it is now possible to systematically associate every Cartesian grid point in the array with the original reflectivity data required to compute an interpolated estimate. This array is saved on disk for access later in Step 2, and may be referenced again in its present configuration for the interpolation of subsequent storm volumes provided that the Cartesian grid system and the original elevation scan sequence remain unchanged from one storm volume to the next.

STEP 2

One by one, all the words in the array described above are read in, unpacked and processed by this step. At each interpolation level reflectivity data from the upper elevation scan is input and held simultaneously in memory with data from the lower scan. A sequential search, increasing in azimuth along the elevation scans, matches the current Cartesian grid point with the four radar beams (two on either side, above and below) surrounding its location in space.

As soon as this match is made, the grid point with spherical coordinates (R,θ,ϕ) is then projected onto the elevation scan above and below it along an arc of constant range in the R, θ plane (i.e., the ϕ direction). A bilinear interpolation along range and azimuth is performed at the projection point on each elevation plane using the four adjacent values of Z_e (Greene, 1970; Miller and Strauch, 1974). This procedure is illustrated in Fig. 2a. The expression used to estimate the value Z_e on a constant elevation plane at projection point (R,θ) is given by

$$\begin{aligned} Z_e(R,\theta) = \frac{1}{\Delta_R \Delta_\theta}\{ &(R-R_i)[(\theta-\theta_j)Z_e(i+1, j+1) \\ &-(\theta-\theta_{j+1})Z_e(i+1, j)] \\ &-(R-R_{i+1})[(\theta-\theta_j)Z_e(i, j+1) \\ &-(\theta-\theta_{j+1})Z_e(i, j)]\}, \end{aligned} \quad (5)$$

where R and θ are the slant range and azimuth of the projection point, Δ_R is the range spacing, and Δ_θ is the angular distance between radar beams θ_j and θ_{j+1}.

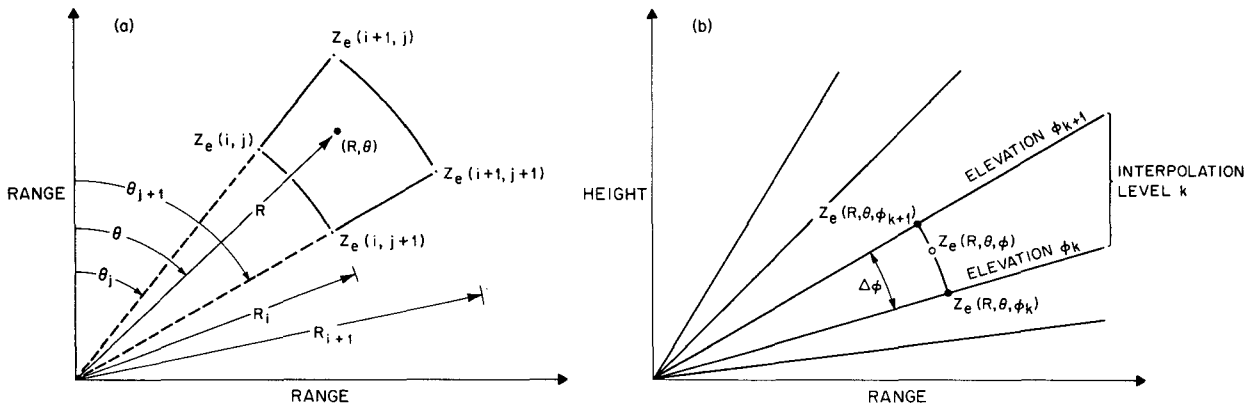

FIG. 2. (a) Sampling grid for bilinear interpolation of Z_e at the projection point R, θ of a Cartesian grid location onto a surface of constant elevation (after Miller and Strauch, 1974). (b) Final estimation of Z_e at Cartesian grid location R, θ, ϕ using interpolated reflectivities from the projection points on constant elevation surfaces ϕ_k and ϕ_{k+1}.

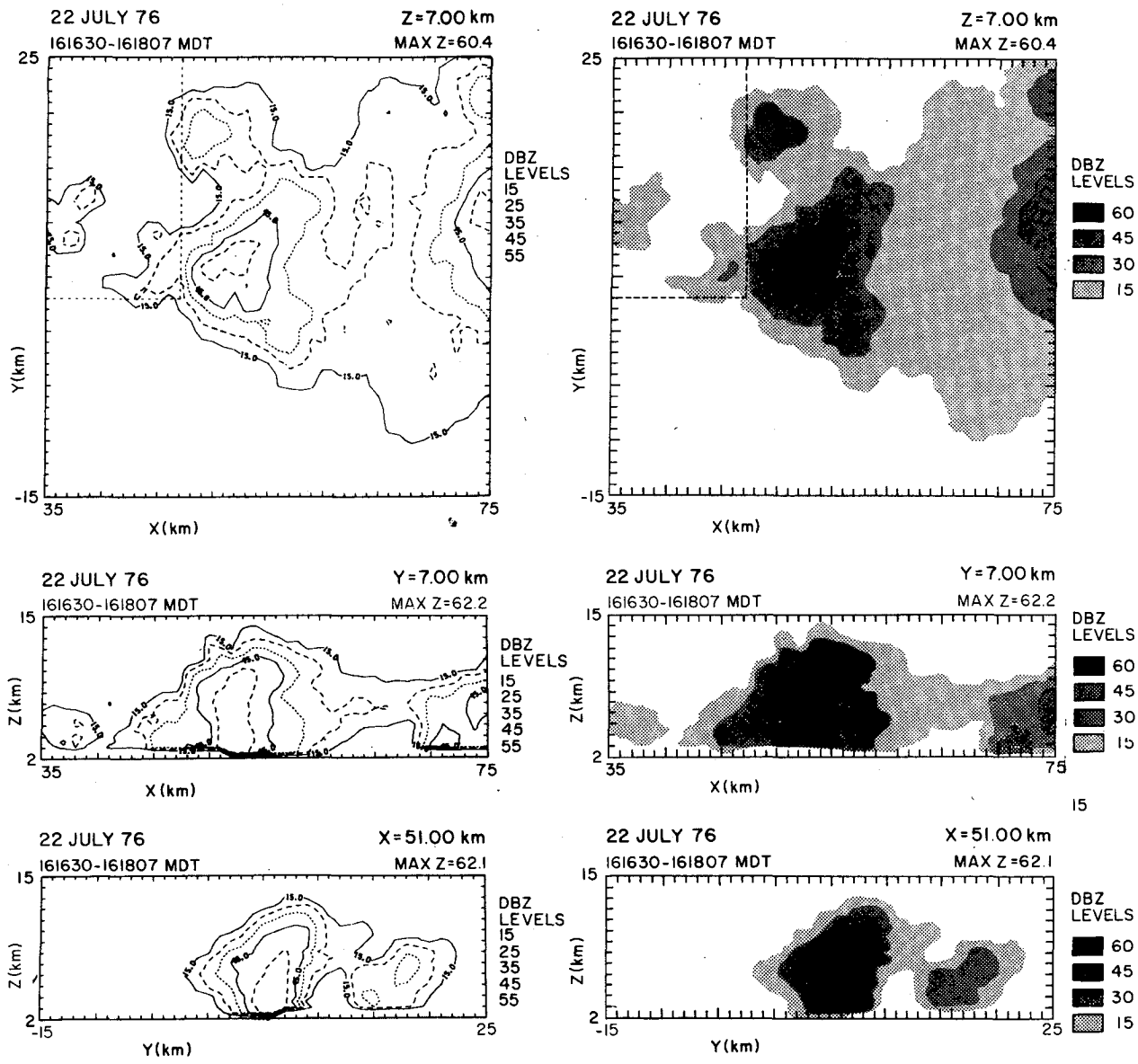

FIG. 3. Orthogonal sections, taken from the same scanned volume, containing interpolated reflectivities (dBZ). Contour and gray-scale plots are shown for a selected Cartesian plane along each spatial dimension. X and Y axes are in kilometers east and north of the radar located near Grover, Colorado. The Z axis is in km MSL. The value of the plane held constant, the reflectivity levels, and other pertinent information appear outside the perimeter of each display. On horizontal sections the dashed interior boundary designates location of dense precipitation network.

To obtain a reflectivity value at the interpolation location (R,θ,ϕ) a final linear interpolation is performed using the estimates at the projected points (R,θ,ϕ_k) and (R,θ,ϕ_{k+1}):

$$Z_e(R,\theta,\phi)=\frac{1}{\Delta\phi}[(\phi-\phi_k)Z_e(R,\theta,\phi_{k+1}) - (\phi-\phi_{k+1})Z_e(R,\theta,\phi_k)], \quad (6)$$

where ϕ is the elevation angle of (R,θ,ϕ) and $\Delta\phi$ the angular distance between elevation scans ϕ_k and ϕ_{k+1}. This final calculation is illustrated in Fig. 2b.

Once $Z_e(R,\theta,\phi)$ has been calculated, the angular coordinates of the interpolation location taken from the 60-bit word will no longer be needed, and the 60-bit word is reconstructed with the following quantities (packed in decreasing order of significance): 1) original indices of the grid point location in Cartesian space, and 2) interpolated value converted to dBZ.

STEP 3

After all interpolation locations have been processed by Step 2, the array of reconstructed computer words is sorted in ascending order thereby restoring the

Cartesian grid system, now associated with reflectivity estimates, to its original structure (most commonly organized in planes of constant z). Further manipulation of the indices followed by sorting of the elements in the array will easily reorganize these grid-point reflectivity estimates into planes of constant y or x.

b. Software limitations and timing

The present system is designed for fast interpolation of severe storm data collected in sector scan mode. In an effort to achieve optimal efficiency when reducing the more typical cases, certain limitations have been imposed on input data and Cartesian grid specifications.

A maximum of 54 000 reflectivity values (number of rays×number of gates per ray) may be supplied as input at each elevation scan with as many as 60 constant elevation scans for a single volume. In order to minimize storage requirements, the input data are specified to be calibrated reflectivity factors in dBZ (12 bits each) packed five per 60-bit word. The Cartesian

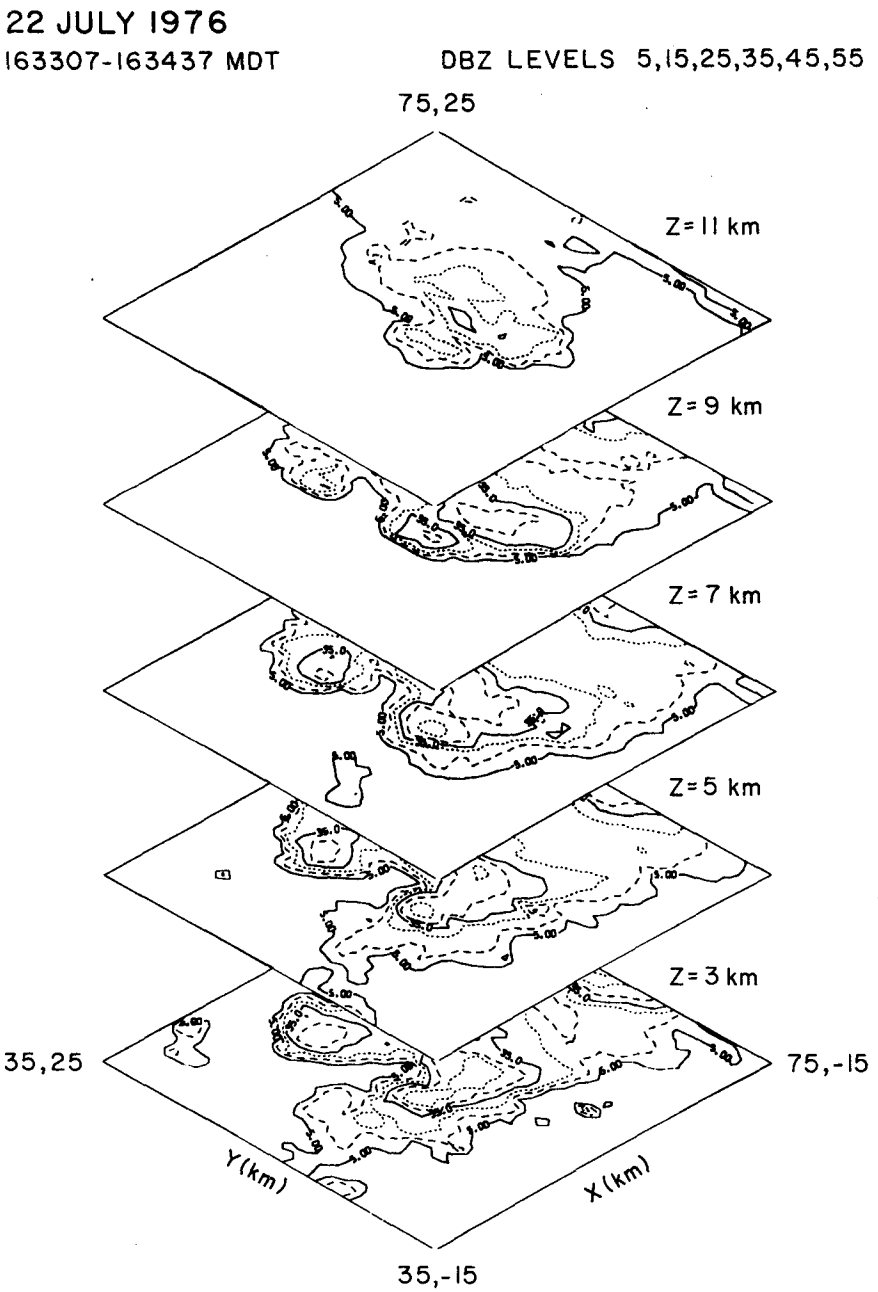

FIG. 4. Projected images of contoured CAPPI planes taken from the same volume. X and Y axes are oriented east and north relative to the radar with corner points marked in kilometers. The level of each CAPPI is given in km MSL.

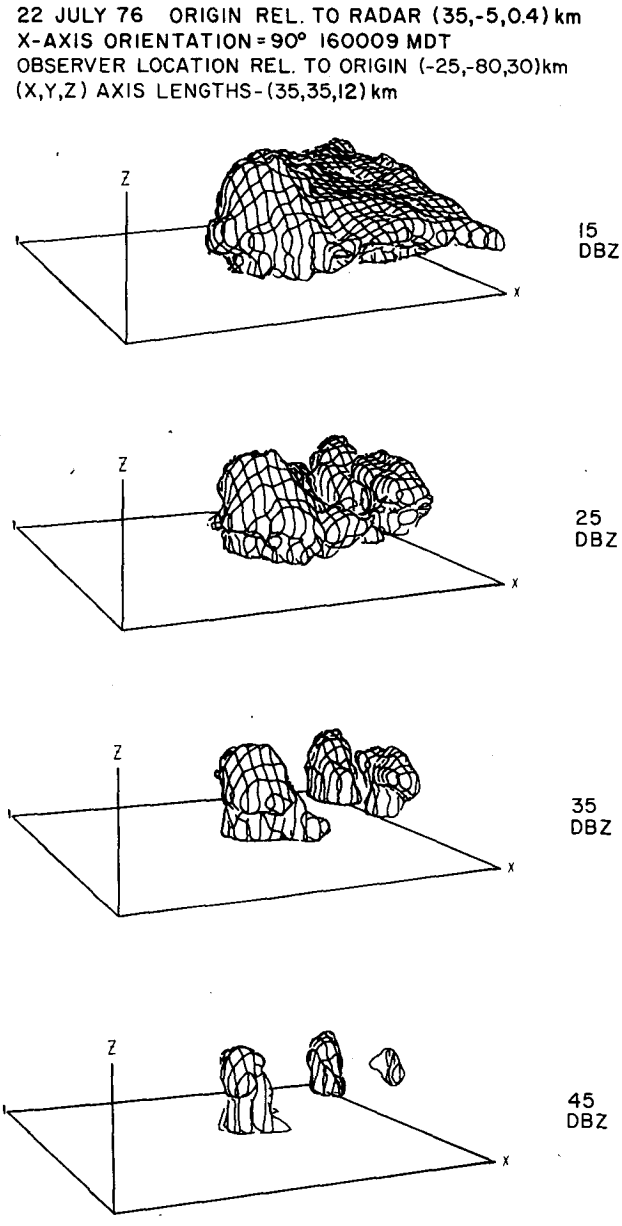

FIG. 5. Perspective displays of surfaces of constant reflectivity with the value of each surface given in dBZ. *X* and *Y* axes are oriented east and north relative to the radar.

coordinate system is defined by the user and may have unique spacing along each axis. It can be located and oriented anywhere in space and may contain up to 144 000 grid-point locations with a maximum of 8000 locations in any orthogonal plane. The only restriction on its placement is that it be located downrange from the radar (i.e., no portion of the Cartesian grid be directly above the radar) so as to limit the sector of input data required for interpolation to a maximum width of 180° along azimuth.

The interpolation procedure, subject to the above limitations, requires approximately 45 000 (60-bit) words of addressable memory on a CDC computer as well as sufficient external access capability for sorting and saving data arrays which exceed the addressable memory of the machine.

Timing tests performed on the NCAR CDC/7600 have demonstrated that the production of orthogonal displays, using this procedure, can be a reasonable alternative (although more likely a supplement) to the generation of PPI's. Scanned volumes were selected, each containing an average of ten elevation sweeps. First, PPI plots were generated from these data covering a 1600 km^2 area. Next these same data were interpolated to a 41×41×25 Cartesian grid (42 025 points with 1 km×1 km×0.5 km resolution) over the same area and contoured plots of all orthogonal sections were produced. Whereas the generation of PPI plots required 6 s computer time for an average volume containing 10 elevation scans, the interpolation and plotting of the 107 (41+41+25) cross sections required an average of 30 s. The interpolation procedure therefore took five times longer, yet produced ten times as many displays.

5. Results of the interpolation

The most useful result of the interpolation procedure is the generation of detailed orthogonal sections containing reflectivity factors which can be displayed using either contour or gray-scale plotting software (see Fig. 3). Other available graphics include projected images of contoured planes (used to construct Fig. 4) and perspective displays of three-dimensional constant reflectivity surfaces (used to construct Fig. 5).

a. Interpolation methodology

An obvious concern is the accuracy of these orthogonal presentations. Within the framework of the system any interpolation scheme utilizing data from two consecutive elevation scans can be readily implemented. However, such a wide range of choices is subsequently restricted by not only the desired properties of the interpolated field but also the nature of the original data.

As outlined earlier, one of the requirements of the interpolation procedure was that it reconstruct, as closely as possible, reflectivity patterns manifest in the original data. Assuming that these original data are indeed accurate, an optimal interpolation scheme would be one operating on the nearest and fewest values that are necessary for preserving continuity in all three dimensions. Under this premise it was concluded that bilinear interpolation using the eight values surrounding a Cartesian location would be the most effective and efficient procedure.

Since both low-elevation PPI's and low-altitude CAPPI's display reflectivity structure from approximately the same region, one technique for verifying the accuracy of any interpolation method is to make

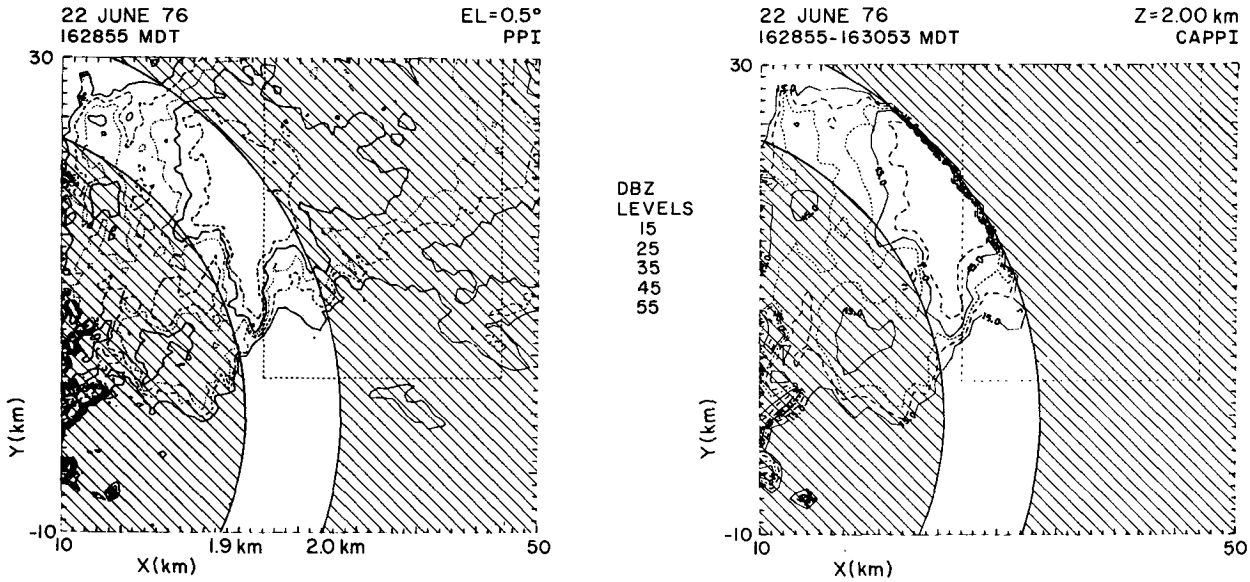

FIG. 6. Comparison between reflectivity patterns in a low-elevation PPI (0.5°) and a low-altitude CAPPI (2.0 km MSL). The region selected for comparison lies between 1.9 and 2.0 km MSL on the constant elevation scan surface. Data outside this region have been stippled. Similar stippling has been added to the CAPPI display. Contour levels (dBZ) are identical for both plots. All other features are similar to those in Fig. 3.

comparisons between these two presentations. Fig. 6 contains an example of such a comparison using severe storm data collected during the 1976 NHRE field season. In this and other cases, close agreement was observed when comparing reflectivity patterns obtained from the original sector scan data with those generated by performing bilinear interpolation on Z_e field values. Although fine-scale structure below the resolution of the Cartesian grid is no longer apparent, it should be noted that general features, such as high-reflectivity cores and steep gradients, have been adequately reconstructed in the interpolated data.

One area of concern which merits further discussion has been whether the interpolation should be performed on units of Z_e or dBZ. Our experience with severe storm data has led us to conclude that, in general, Z_e interpolation tends to overestimate the lower reflectivities and more closely approximate the higher values (>35 dBZ). In the case of dBZ interpolation the opposite is true: closer approximation of lower values is achieved at the expense of underestimating the higher reflectivities.

Fig. 7 contains two different displays of the same vertical cross section. The upper figure was generated by performing the interpolation on units of Z_e, while the bottom figure was produced using the same procedure on units of dBZ. In examining the bottom figure lowered peak reflectivity, diminished areal coverage at each contour level and broadened gradients can be observed. Such features are indicative of the systematic differences between these two approaches and should be given serious consideration before converting any data set to Cartesian coordinates. For instance, in those situations where emphasis is on preserving the spatial structure of minimum detectable signals and other low-reflectivity features, dBZ field interpolation may produce more desirable results. However, when working with fine-resolution radar data collected from severe storms, primary concerns might be the identification of high-reflectivity cores and the preser-

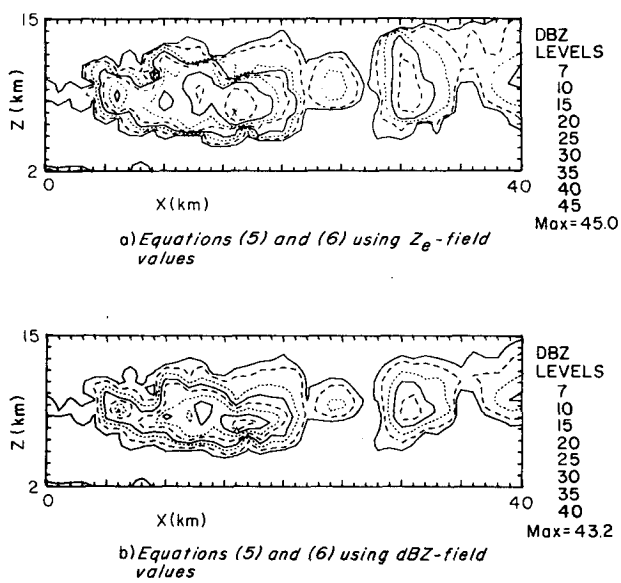

FIG. 7. Contour display of the same interpolated vertical cross section. The upper figure was generated by performing the interpolation on units of Z_e; the lower, on units of dBZ. Orientation of the cross section is west to east. The X axis origin is located 10 km east of the radar.

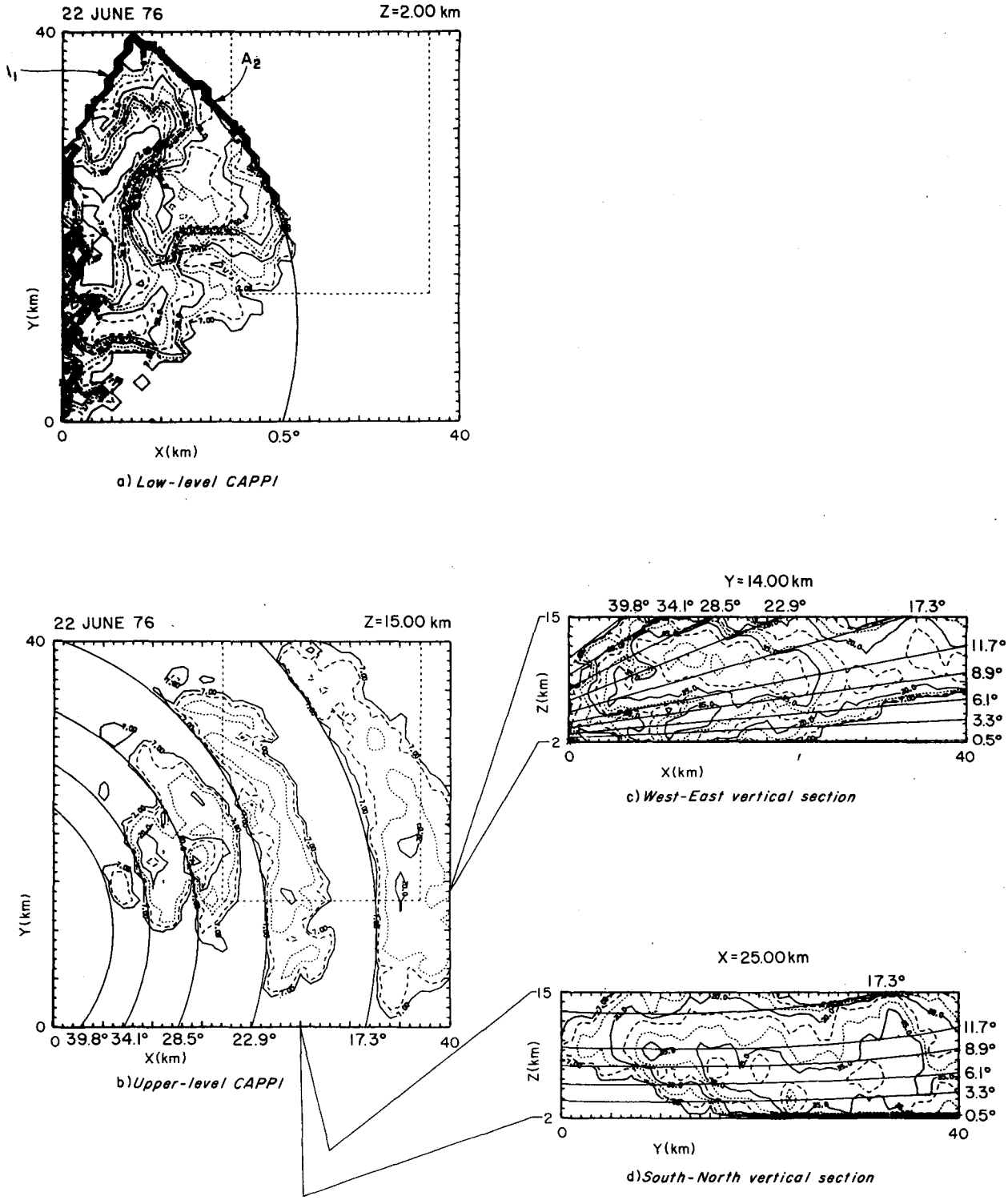

FIG. 8. Contour displays of orthogonal sections containing examples of artifacts in the interpolated reflectivity structure. These cross sections have been selected from the same Cartesian volume. Lines of intersection with the original elevation scans have been superimposed and angles specified. The X axis origin is located 10 km east of the radar, Y axis origin 10 km south.

vation of maximum reflectivity. Under these circumstances preference may be given to the Z_e field interpolation method.

Understandably, there is no interpolation method which produces the best results for all cases. Each investigator, depending on his or her requirements,

ultimately decides which interpolation scheme generates the most "realistic" product. Accordingly, it is not the function of this system to make that decision, but rather to provide the capability for experimentation with a reasonable set of choices. Presently, the system is designed to perform an 8-point bilinear interpolation using either Z_e field or dBZ field values in conjunction with various extrapolation options for the treatment of data at echo boundaries. As experience is gained, more schemes are certain to be incorporated.

b. Potential artifacts

Identifiable artifacts may appear in the interpolated data when all Cartesian grid points are not located within the scanned volume of the radar and in those regions where the spatial resolution of the original data is coarse. Fig. 8 presents examples of artifacts which have been encountered.

1) Grid points outside the scanned volume

Fig. 8a contains artifacts in a CAPPI section occurring because all grid-point locations were not within the total volume scanned. In the case of artifact A_1, the azimuth scanning did not continue to the actual limits of the storm echo and the truncation of reflectivity patterns along the radial is obvious. Artifact A_2 appears because the *lowest* elevation scan intersects the CAPPI, causing those points below the arc of intersection to be excluded from the interpolation. This artifact also manifests itself in the vertical sections at lower altitudes, especially where the Cartesian grid is distant from the radar. Truncation of reflectivity patterns at the lowest height in Fig. 8d is a representative example of this effect.

2) Course spatial resolution in the original data

Figs. 8b–8d are all taken from the same interpolated volume and contain artifacts caused by a large separation between higher elevation scans in the original data. As in Fig. 8a, lines of intersection with the elevation scan planes have been added and their angles specified.

The interpolation method preserves continuity along arcs of constant radius. As resolution decreases and as the angular difference between the original radials and the Cartesian planes approaches 45°, discontinuities appear in the orthogonal sections. These discontinuities become obvious where the limits of the echo typically occur in an orthogonal plane, such as along the top of a storm. Fig. 9 illustrates how discontinuities are generated under these conditions. An idealized storm with a flat top and continuous 15 dBZ reflectivity is sampled at a high elevation angle with coarse resolution between consecutive scans. Approximate interpolated values are indicated along the horizontal plane. When examining actual data collected under the same conditions, it can be seen that these discontinuities mainfest themselves as annular patterns in upper level CAPPI's (Fig. 8b); whereas, in vertical sections (Figs. 8c, 8d) a sawtooth effect is observed along the top of the storm.

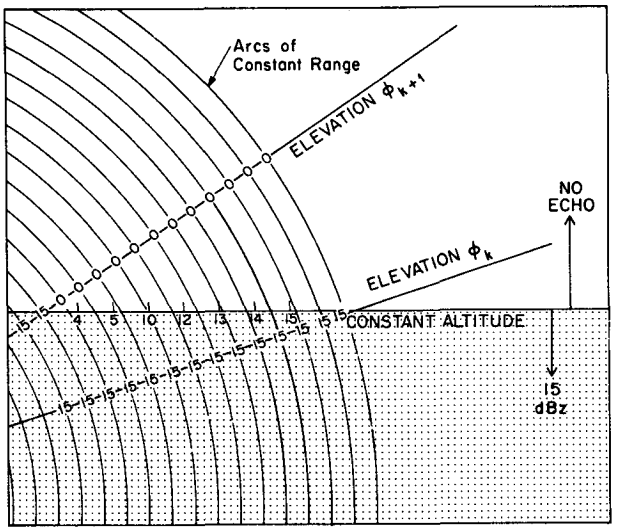

FIG. 9. Idealized situation demonstrating how artifacts are generated when sampling angle is high and scan resolution is poor, such as along the top of a storm. Stippled area denotes region of continuous 15 dBZ return. In the no echo region the minimum detectable signal is 0 dBZ. Sampled reflectivities are given along the beams at each gate. Fictitious values resulting from interpolation are indicated along the constant altitude plane.

Although these artifacts most commonly appear at storm top due to large angular steps between consecutive elevation scans, it is entirely possible for them to occur under similar circumstances at the sides of storms as a result of poor resolution along azimuth. The example chosen in Fig. 8 is an extreme one, but it should alert any potential user that caution is required when interpolating in data sparse regions. In general, artifacts are likely to be generated in any region of the storm where the resolution of the interpolated field is substantially higher than that of the original data.

Efforts have been made to objectively recreate reflectivity patterns at storm top under conditions of poor resolution, none of which have proven successful. Modification of the interpolation scheme to exclude minimum reflectivity values under these conditions causes extrapolation of higher reflectivities into echo-void regions without eliminating the artifacts. Manipulation of the weighting procedure to effect a faster dropoff of reflectivity at echo boundaries also preserves the artifacts while causing the storm to shrink around the edges. More elaborate interpolation schemes were examined and as the degree of sophistication increased the artifacts became smoother, but they never disappeared. The best approach in dealing with these artifacts is to leave them alone. They are caused by inadequate resolution in the measurement system and any objective technique which attempts to generate

plausible reflectivity patterns in data-sparse regions will probably end up disguising these artifacts instead of eliminating them.

6. Summary and conclusions

This paper has presented a system for the interpolation and display of reflectivity factor data in three-dimensional space. The basic algorithm was designed so that only one systematic pass through the original data is required to complete the interpolation process. As a result, the software package is efficient in its expenditure of computer time and allocation of storage. This has enabled the economic presentation of reflectivity factor data on orthogonal planes generated from large amounts of data collected in PPI scan mode.

Although emphasis has been placed on preserving the features and continuity of the original data, artifacts may appear in areas where scan resolution is poor. In most cases such artifacts are easy to identify and observations from independent sources may be required to construct representative echo patterns in those regions.

Analysis of three-dimensional storm structure is significantly easier when reflectivity estimates are readily available in a Cartesian coordinate system. Contoured and grey-scale plots of data in orthogonal planes are a typically useful product; perspective displays of constant reflectivity surfaces in a volume are also practical. The presence of data in common coordinates also facilitates the construction of more sophisticated presentations such as those depicting echo evolution across time and space.

Acknowledgments. The authors would like to acknowledge the scientific staff of the National Hail Research Experiment for their support throughout the development of the software. Special thanks are due Mr. J. C. Fankhauser, Mr. R. E. Rinehart, and Drs. F. I. Harris, C. A. Knight and G. B. Foote, all of whom made fundamental contributions to the final form of the manuscript. Particular thanks also go to Charlene Limon and Barb Strand for preparing this document, to Mr. S. Connolly, Mr. B. Hemphill and Mr. L. Fortier for the figure drafting, and to Mrs. B. Toland for her able efforts in reducing the data. Lastly, we would like to acknowledge Mr. Thomas Wright and Mr. David Robertson of the NCAR computing facility for the existence of the excellent graphics software which was used to generate the displays.

REFERENCES

Battan, L. J., 1973: *Radar Observation of the Atmosphere*, rev. ed. The University of Chicago Press, 324 pp.

Boardman, J. H., and P. L. Smith, Jr., 1974: A computer-generated four-dimensional graphic display for weather radar data. *Bull. Amer. Meteor. Soc.*, **55**, 16–19.

Eccles, P. J., 1975: Developments in radar meteorology in the National Hail Research Experiment to 1973. *Atmos. Tech.*, No. 6, NCAR, 34–35.

Greene, D. R., 1971: Numerical techniques for the analysis of digital radar data with applications to meteorology and hydrology. Ph.D. dissertation, Texas A & M University, 125 pp.

Heymsfield, G. M., 1976: Statistical objective analysis of dual-doppler radar data from a tornadic storm. *J. Appl. Meteor.*, **15**, 59–68.

Kessler E., III, and J. A. Russo, Jr., 1963: A program for the assembly and display of radar-echo distributions. *J. Appl. Meteor.*, **2**, 582–593.

Kohn, N. M., A. L. Johnston and C. G. Mohr, 1978: MUDRAS-Multiple doppler radar analysis system. NOAA Tech. Memo. ERL WPL-35, Wave Propagation Laboratory, Boulder, 170 pp.

Lhermitte, R. M., and M. Gilet, 1976: Acquisition and processing of tri-Doppler radar data. *Preprints 17th Radar Meteorology Conf.*, Seattle, Amer. Meteor. Soc., 1–6.

Marshall, J. S., 1957: The constant-altitude presentation of radar weather patterns. *Preprints 6th Radar Meteorology Conf.*, Cambridge, Amer. Meteor. Soc., 321–324.

Miller, L. J., and R. G. Strauch, 1974: A dual-Doppler radar method for the determination of wind velocities within precipitating weather systems. *Remote Sens. Environ.*, **3**, 219–235.

Ray, P. S., K. K. Wagner, K. W. Johnson, J. J. Stephens, W. C. Bumgarner and E. A. Mueller, 1978: Triple-Doppler observations of a convective storm. *J. Appl. Meteor.*, **17**, 1201–1212.